

Function Trees: Transparent Machine Learning

Jerome H. Friedman*

March 21, 2024

Abstract

The output of a machine learning algorithm can usually be represented by one or more multivariate functions of its input variables. Knowing the global properties of such functions can help in understanding the system that produced the data as well as interpreting and explaining corresponding model predictions. A method is presented for representing a general multivariate function as a tree of simpler functions. This tree exposes the global internal structure of the function by uncovering and describing the combined joint influences of subsets of its input variables. Given the inputs and corresponding function values, a function tree is constructed that can be used to rapidly identify and compute all of the function's main and interaction effects up to high order. Interaction effects involving up to four variables are graphically visualized.

1 Introduction

A fundamental exercise in machine learning is the approximation of a function of several to many variables given values of the function, often contaminated with noise, at observed joint values of the input variables. The result can then be used to estimate unknown function values given corresponding inputs. The goal is to accurately estimate the underlying (non noisy) outcome values since the noise is by definition unpredictable. To the extent that this is successful the estimated function may, in addition, be used to try to understand underlying phenomena giving rise to the data. Even when prediction accuracy is the dominate concern, being able to comprehend the way in which the input variables are jointly combining to produce predictions may lead to important sanity checks on the validity of the function estimate. Besides accuracy, the success of this latter exercise requires that the structure of the function estimate be represented in a comprehensible form.

It is well known, and often commented, that the most accurate function approximation methods to date tend not to provide comprehensible results. The function estimate is encoded in an obtuse form that obscures potentially recognizable relationships among the inputs that give rise to various function output values. This is especially the case when the function is not inherently low dimensional. That is, medium to large subsets of the input variables act together to influence the function $F(\mathbf{x})$ in the sense that their combined contribution cannot be represented by a combination of smaller subsets of those variables (interaction effects). This has led to incomplete interpretations based on low dimensional approximations such as additive modeling with no interactions, or models restricted to at most two-variable interactions.

2 Interaction effects

For input variables $\mathbf{x} = (x_1, x_2, \dots, x_p)$ a function $F(\mathbf{x})$ is said to exhibit an interaction between two of them x_j and x_k if the difference in the value of $F(\mathbf{x})$ as result of changing the value of one of them x_j depends on the value of the other x_k . This means that in order to understand the

*Department of Statistics, Stanford University, Stanford, CA 94305, USA. (jhf@stanford.edu)

effect of these two variables on $F(\mathbf{x})$ they must be considered together and cannot be studied separately. An interaction effect between variables x_j and x_k implies that the second derivative of $F(\mathbf{x})$ jointly with respect to x_j and x_k is not zero for at least some values of \mathbf{x} . That is,

$$E_{\mathbf{x}} \left[\frac{\partial^2 F(\mathbf{x})}{\partial x_j \partial x_k} \right]^2 > 0, \quad (1)$$

with an analogous expression involving finite differences for categorical variables. If there is no interaction between these variables, the function $F(\mathbf{x})$ can be expressed as a sum of two functions, one that does not depend on x_j and the other that is independent of x_k

$$F(\mathbf{x}) = f_{\setminus j}(\mathbf{x}_{\setminus j}) + f_{\setminus k}(\mathbf{x}_{\setminus k}). \quad (2)$$

Here $\mathbf{x}_{\setminus j}$ and $\mathbf{x}_{\setminus k}$ respectively represent all variables except x_j and x_k . If a given variable x_j interacts with no other variable, then the function can be expressed as

$$F(\mathbf{x}) = f_j(x_j) + f_{\setminus j}(\mathbf{x}_{\setminus j}) \quad (3)$$

where the first term on the right is a function only of x_j and the second is independent of x_j . In this case $F(\mathbf{x})$ is said to be “additive” in variable x_j and the univariate function $f_j(x_j)$ can be examined to study the effect of x_j on the function $F(\mathbf{x})$ independently from the effects of the other variables.

Higher order interactions are analogously defined. A function $F(\mathbf{x})$ is said to have an n -variable interaction effect involving variables $\{x_j\}_1^n$ if

$$E_{\mathbf{x}} \left[\frac{\partial^n F(\mathbf{x})}{\partial x_1 \partial x_2 \cdots \partial x_n} \right]^2 > 0, \quad (4)$$

again with an analogous expression involving finite differences for categorical variables. The existence of such an n -variable interaction implies that the effect of the corresponding variables $\{x_j\}_1^n$ on the function $F(\mathbf{x})$ cannot be decomposed into a sum of functions each involving subsets of those variables. If there is no such interaction, the contribution of variables $\{x_j\}_1^n$ to the variation of $F(\mathbf{x})$ can be decomposed into a sum of functions each not depending upon one of these respective variables

$$F(\mathbf{x}) = \sum_{j=1}^n f_{\setminus j}(\mathbf{x}_{\setminus j}). \quad (5)$$

If none of the variables in a subset $s = \{x_j\}_1^n$ interact with any of the variables in its complement set $\setminus s = \{x_j\}_{n+1}^p$, then the function is additive in the variable subset s

$$F(\mathbf{x}) = f_s(\mathbf{x}_s) + f_{\setminus s}(\mathbf{x}_{\setminus s}) \quad (6)$$

and one can study the effect of $\{x_j\}_1^n$ on the function $F(\mathbf{x})$ separately from that of the other variables.

The notion of interaction effects can be useful for understanding a function $F(\mathbf{x})$ if it is dominated by those of low order involving variable subsets $s \subset \{x_j\}_1^p$ with small cardinality ($|s| \ll p$). In this case a target function of many variables can be understood in terms of a collection of lower dimensional functions each depending on a relatively small different subset of the variables. It is generally easier to comprehend the lower dimensional structure associated with fewer variables. Also, a common regularization method is to more heavily penalize or forbid solutions involving higher order interactions. Although often useful, this can result in lower accuracy and/or misleading interpretations when $F(\mathbf{x})$ involves substantial interaction effects of higher order than that assumed. As seen below the existence of such higher order interactions can mislead interpretation by causing the functional form of those of lower order to depend on values of other unknown variables.

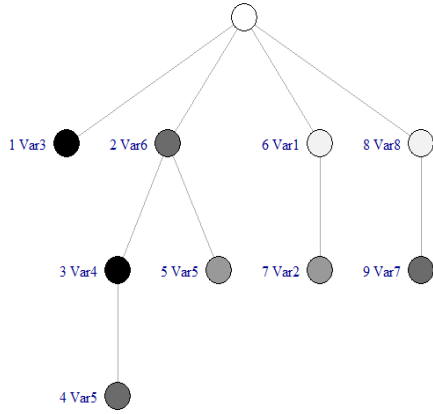


Figure 1: Function tree.

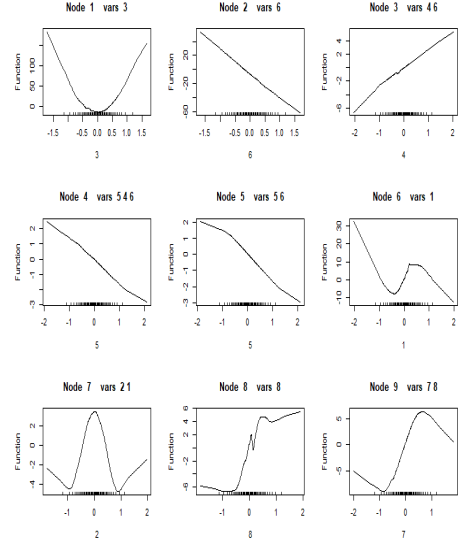


Figure 2: Node functions.

3 Function trees

A function tree is a way of representing a multivariate function so as to uncover and estimate its interaction effects of various orders. The input function $F(\mathbf{x})$ is defined by data $\{\mathbf{x}_i, y_i\}_1^N$ with \mathbf{x} representing multivariate evaluation points and y the corresponding function values perhaps contaminated with noise. The output of the procedure is a set of univariate functions, each one depending on a single selected input variable. These functions are arranged as the non root nodes of a tree. A constant function is associated with the root. The tree provides a prescription for combining these univariate functions to form the multivariate function approximation $\hat{F}(\mathbf{x})$.

Figure 1 shows one such function tree derived from simple simulated data for illustration. Figure 2 shows the nine non constant functions corresponding to each of the respective non root nodes of the tree. In addition to its associated univariate function (Fig. 2), each tree node k represents a basis function $B_k(\mathbf{x})$. The sum of these basis functions forms the final multivariate approximation

$$\hat{F}_K(\mathbf{x}) = B_0 + \sum_{k=1}^K B_k(\mathbf{x}). \quad (7)$$

Each node's basis function is the product of its associated univariate function and those of the nodes on the path from it to the root

$$B_k(\mathbf{x}) = \prod_{l \in p(k)} f_l(x_{j(l)}). \quad (8)$$

Here $p(k)$ represents those nodes l on the path from node k to the root and $j(l)$ labels the input variable associated with each such node l . The darkness of each node's shading in Fig. 1 corresponds to the estimated relative influence of its basis function on the final function estimate as measured by its standard deviation over the training data.

The interaction level of each basis function (8) is the number of univariate functions of *different* variables along the path from its corresponding node to the root of the tree. Products of univariate functions involving n different variables satisfy (4). Note that different univariate functions of the *same* variable may appear multiple times along the same path. While potentially

improving the model fit they do not increase interaction level. With this approach interactions among a specified subset of the variables s are modeled by sums of products of univariate functions of those variables

$$J_s(\{x_j\}_{j \in s}) = \sum_{k=1}^{K_s} \prod_{j \in s} f_{jk}(x_j). \quad (9)$$

The function tree model shown in Figs. 1 & 2 was obtained by applying the procedure described below to a simulated data example. There are 10000 observations with outcome variables generated as $y = F(\mathbf{x}) + \varepsilon$ with $\mathbf{x} \sim N^8(0, 0.5)$ and

$$F(\mathbf{x}) = 4 \sin(\pi x_1) \cos(\pi x_2) + 7 x_3^2 + 15 (x_4 + 0.4) (x_5 - 0.6) (x_6 + 0.2) + 5 \sin(\pi (x_7 + 0.1) x_8). \quad (10)$$

The noise is generated as $\varepsilon \sim N(0, \text{var}(F)/4)$ producing a 2/1 signal/noise ratio. This target function has an additive dependence on the third variable x_3 , separate two-variable interactions between (x_1, x_2) and (x_7, x_8) respectively, and a trilinear three-variable interaction among (x_4, x_5, x_6) .

The first node of the tree is seen to incorporate the pure additive effect of x_3 . Nodes 2 - 5 model the (x_4, x_5, x_6) three-variable interaction. The two-variable interaction between x_1 and x_2 is modeled by nodes 6 and 7, and that of x_7 and x_8 is modeled by nodes 8 and 9. The nine univariate functions (Fig. 2) combined as specified by the tree (Fig. 1) produce a multivariate function that explains 97% of the variance of the target (10).

3.1 Tree construction

Function trees are constructed in a standard forward stepwise best first manner. Initially the tree consists of a single root node representing a constant function B_0 . At the K th step there are K basis functions (7) (8) in the current model $\hat{F}_K(\mathbf{x})$. The $(K + 1)$ st is taken to be

$$B_{K+1}(\mathbf{x}) = B_{k^*}(\mathbf{x}) f^*(x_{j^*}) \quad (11)$$

where j^* , k^* , and f^* are the solution to

$$(j^*, k^*, f^*) = \arg \min_{(j, k, f)} \hat{E} \left(y - \hat{F}_K(\mathbf{x}) - B_k(\mathbf{x}) f(x_j) \right)^2. \quad (12)$$

Here $B_k(\mathbf{x})$ is one of the basis functions in the current model, $f(x_j)$ is a function of one of the predictor variables x_j and the empirical expected value is over the data distribution. The model is then updated

$$\hat{F}_{K+1}(\mathbf{x}) = \hat{F}_K(\mathbf{x}) + B_{k^*}(\mathbf{x}) f^*(x_{j^*}) \quad (13)$$

for the next iteration. In terms of tree construction the update consists of adding a daughter node to current node k^* with associated function $f^*(x_{j^*})$. Iterations continue until the goodness-of-fit stops improving as measured on an independent test data sample.

3.2 Backfitting

As with all tree based methods, smaller trees (less nodes) tend to be more easily understood. Here tree size can be reduced and accuracy improved by increased function optimization (backfitting) at each step (Friedman and Stuetzle 1981). This is implemented here by updating the functions associated with all current tree nodes in presence of the newly added one, and those previously updated. In particular, after adding the new $(K + 1)$ st node, all node functions are re-estimated $f_k(x_{j(k)}) \leftarrow f_k^*(x_{j(k)})$ one at a time in order starting from the first

$$f_k^*(x_{j(k)}) = \arg \min_{\tilde{f}} \hat{E}_{\mathbf{x}} \left[y - \hat{F}_{K+1}(\mathbf{x}) - B_k(\mathbf{x}) \left(\tilde{f}(x_{j(k)}) / f_k(x_{j(k)}) - 1 \right) \right]^2, \quad (14)$$

$$\hat{F}_{K+1}(\mathbf{x}) \leftarrow \hat{F}_{K+1}(\mathbf{x}) + B_k(\mathbf{x}) (f^*(x_{j(k)})/f_k(x_{j(k)}) - 1), k = 1, 2, \dots, (K + 1). \quad (15)$$

Here k labels a node of the tree and f_k its associated function of variable $x_{j(k)}$. In terms of tree construction, each such step involves replacing each (k th) node’s current function $f_k(x_{j(k)})$ with $f_k^*(x_{j(k)})$ (14). No changes are made to tree topology (Fig. 1) or the input variables associated with each node. Only the functions (Fig. 2) are updated. Backfitting passes can be repeated until the model becomes stable. This usually happens after one or two passes. Note that in the presence of backfitting function tree models are not nested. All of the basis functions of the $K + 1$ node model are different from those of its K node predecessor.

3.3 Univariate function estimation

The central operation of the above procedure is repeated estimation of univariate functions of the individual predictor variables. In both (12) and (14) the solutions take the form of weighted conditional expectations

$$\hat{f}(x_j) = \hat{E}_{w^2} \left[\frac{r}{w} \mid x_j \right], \quad (16)$$

where w represents one of the current basis functions $w = B_k(\mathbf{x})$ and $r = y - \hat{F}(\mathbf{x})$ are the current residuals. The function tree procedure as described above is agnostic concerning the methods used for this estimation. However, actual performance in terms of execution speed and prediction accuracy can be highly dependent on such choices.

A major consideration in the choice of an estimation method for a particular variable x_j is the nature of that variable in terms of the values it realizes, and connections between those values. A categorical variable (factor) realizes discrete values with no order relation. The only method for evaluating (16) for such variables is to take the weighted (w^2) mean of r/w at each discrete x value. This is also a viable strategy if the x_j values are orderable but realize only a small set of distinct values.

For numeric variables that realize many distinct orderable values one can take advantage of the presumed smoothness of the solution function to improve accuracy by borrowing strength from similarly valued observations. There are many such methods for “smoothing” data (see Irizarry 2019). For the examples presented below near neighbor local averaging and local linear fitting were employed. Near neighbor local averaging estimates are equivariant under monotone transformations of the x -values, depending only their relative ranks. This can provide higher accuracy in the presence of irregular or clumped x -values, immunity to x outliers, resistance to y outliers and more cautious (constant) extrapolation at the edges. For more evenly distributed data with many distinct x -values, in the absence of x and y outliers, local linear fitting can yield smoother more accurate results.

4 Interpretation

The primary goal of the function tree representation is to enhance interpretation by exposing a function’s separate interaction effects of various orders. These can then be studied using graphical and other methods to gain insight into the nature of the relationship between the predictor variables $\mathbf{x} = (x_1, x_2, \dots, x_p)$ and the target function $F(\mathbf{x})$.

4.1 Partial dependence functions

One way to estimate the contribution of subsets of predictor variables to a function $F(\mathbf{x})$ is through partial dependence functions (Friedman 2001). Let \mathbf{z} represent a subset of the predictor variables $\mathbf{z} \subset \mathbf{x}$ and $\tilde{\mathbf{z}}$ the complement subset $\mathbf{z} \cup \tilde{\mathbf{z}} = \mathbf{x}$. Then the partial dependence of a function $F(\mathbf{x})$ on \mathbf{z} is defined as

$$PD(\mathbf{z}) = E_{\tilde{\mathbf{z}}} [F(\mathbf{x})]. \quad (17)$$

Conditioned on joint values of the variables in \mathbf{z} , the value of the function $F(\mathbf{x})$ is averaged over the joint values of the complement variables $\tilde{\mathbf{z}}$. Since the joint locations of partial dependence functions are generally not identifiable, they are each centered to have zero mean value over the data distribution of \mathbf{x} .

If for a function $F(\mathbf{x})$ the variables in the specified subset \mathbf{z} do not participate in interactions with variables in $\tilde{\mathbf{z}}$ then the additive dependence (6) of $F(\mathbf{x})$ on \mathbf{z} is well defined and given by $PD(\mathbf{z})$. If this is not the case, then the dependence of the target function $F(\mathbf{x})$ on the subset \mathbf{z} is not well defined in the sense that its functional form changes with changing values of the variables in $\tilde{\mathbf{z}}$. In this case one can define a “nominal” dependence by averaging over some distribution $p(\mathbf{x})$ of the predictor variables \mathbf{x} . This confounds the properties of the actual target function $F(\mathbf{x})$ with those of the data distribution $p(\mathbf{x})$ on the resulting estimate of the dependence on \mathbf{z} . Two popular choices for $p(\mathbf{x})$ are the training data and the product of its marginals (independence). Partial dependence functions choose a compromise in which the variables in \mathbf{z} are taken to be independent of those in $\tilde{\mathbf{z}}$. Note that the result between this and using the training data distribution is different only if there are substantial correlations or associations between the interacting variables in \mathbf{z} and $\tilde{\mathbf{z}}$.

Partial dependence functions (17) can be estimated from the data in a straightforward way by evaluating

$$\widehat{PD}(\mathbf{z}) = \frac{1}{N} \sum_{i=1}^N F(\mathbf{z}, \tilde{\mathbf{z}}_i) \quad (18)$$

over a representative set of joint values of \mathbf{z} . This requires $N \cdot N_{\mathbf{z}}$ target function evaluations where $N_{\mathbf{z}}$ is the number of evaluation points and N is the sample size used for averaging.

With the function tree representation partial dependence functions can be computed much more rapidly. For the purpose of computing a partial dependence function on a variable subset \mathbf{z} the function tree model can be expressed as

$$\hat{F}(\mathbf{x}) = A + \sum_{k=1}^K f_k(\mathbf{z}) \cdot g_k(\tilde{\mathbf{z}}) \quad (19)$$

where A represents all basis functions not involving any variables in \mathbf{z} , $f_k(\mathbf{z})$ are functions involving variables only in \mathbf{z} , and $\tilde{\mathbf{z}}$ represents the complement variables. With this representation the partial dependence of $\hat{F}(\mathbf{x})$ on the variables \mathbf{z} is simply

$$\widehat{PD}(\mathbf{z}) = \sum_{k=1}^K \bar{g}_k \cdot f_k(\mathbf{z}) \quad (20)$$

where $\bar{g}_k = \hat{E}_{\mathbf{x}}[g_k(\tilde{\mathbf{z}})]$ is the mean of $g_k(\tilde{\mathbf{z}})$ over the data. This (20) is a particular linear combination of the functions $\{f_k(\mathbf{z})\}_1^K$. The number of target function $\hat{F}(\mathbf{x})$ evaluations required to compute (20) is proportional to

$$C(N, N_{\mathbf{z}}) = N_{\mathbf{z}} + \alpha(\mathbf{z}, \tilde{\mathbf{z}}) \cdot N \quad (21)$$

where $\alpha(\mathbf{z}, \tilde{\mathbf{z}})$ is the fraction of node basis functions (8) involving variables in both \mathbf{z} and $\tilde{\mathbf{z}}$.

4.2 Partial association functions

Partial dependence functions focus on the properties of the function $F(\mathbf{x})$ by averaging over a distribution in which the \mathbf{z} variables are independent of those in $\tilde{\mathbf{z}}$. This concentrates on the target function by removing the effects of associations between those variable subsets. As a result the calculation can sometimes emphasize \mathbf{x} -values for which the data density $p(\mathbf{x})$ is small leading to potential inaccuracy. This only affects a partial dependence to the extent that there are variables in $\tilde{\mathbf{z}}$ with which its variables \mathbf{z} both interact and are correlated.

The function tree representation provides a method for detecting and measuring the strength of such occurrences. “Partial association” functions are defined as

$$\widehat{PA}(\mathbf{z}) = \sum_{k=1}^K f_k(\mathbf{z}) \cdot h_k(\mathbf{z}) \quad (22)$$

where

$$h_k(\mathbf{z}) = E_{\mathbf{x}}[g_k(\tilde{\mathbf{z}}) | f_k(\mathbf{z})] \quad (23)$$

with the functions $f_k(\mathbf{z})$ and $g_k(\tilde{\mathbf{z}})$ defined in (19). As with partial dependence functions (20) this can be viewed as a linear combination of the functions $\{f_k(\mathbf{z})\}_1^K$ but with varying coefficients $\{h_k(\mathbf{z})\}_1^K$ that account for the associations between the variables in \mathbf{z} and the complement variables $\tilde{\mathbf{z}}$. The coefficient functions $h_k(\mathbf{z})$ can be estimated by any univariate smoother. Regression splines with knots at the 20 percentiles are used in the examples below. Note that from (19) partial association functions (22) (23) reduce to partial dependence functions (20) when variables in \mathbf{z} do not participate in interactions with variables in $\tilde{\mathbf{z}}$ ($g_k(\tilde{\mathbf{z}}) = 1$), or they are independent of those in $\tilde{\mathbf{z}}$ with which they do interact ($h_k(\mathbf{z}) = \bar{g}$). Otherwise they can produce different results caused by the variation in the respective coefficient functions $h_k(\mathbf{z})$ induced by the associations between the corresponding interacting variables in \mathbf{z} and $\tilde{\mathbf{z}}$.

Partial association functions can be used to access the influence that associations among the predictor variables have on the corresponding partial dependences. In particular, one can substitute them (22) (23) for partial dependence functions (20) in any analysis. Similar results indicate that such influences are small.

4.3 Interaction detection

Partial dependence functions can be used to detect interaction effects between variables. For example, if a target function $F(\mathbf{x})$ contains no interaction between variables x_j and x_k its partial dependence on those variables is

$$PD(x_j, x_k) = PD(x_j) + PD(x_k) \quad (24)$$

(Friedman and Popescu 2008). If there is such an interaction, $PD(x_j) + PD(x_k)$ represents the additive component and

$$I(x_j, x_k) = PD(x_j, x_k) - PD(x_j) - PD(x_k) \quad (25)$$

represents the corresponding pure interaction component of the effect of x_j and x_k on $F(\mathbf{x})$ as reflected by its partial dependences.

More generally, the pure interaction effect involving variables $s = \{x_j\}_1^n$ is defined to be

$$I(s) = PD(s) - \sum_{u \subset s} I(u) \quad (26)$$

where $I(u)$ is recursively defined as

$$I(u) = PD(u) - \sum_{v \subset u} I(v). \quad (27)$$

This pure interaction component $I(\{x_j\}_1^n)$ is its corresponding partial dependence with all lower order interactions among all its variable subsets removed. If there is no n -variable interaction effect involving $\{x_j\}_1^n$ its pure interaction component $I(\{x_j\}_1^n) = 0$. Note that this result depends only on the properties of the function $F(\mathbf{x})$ (5) and not on the data distribution $p(\mathbf{x})$. The strength of such an interaction effect can be taken to be the standard deviation of its pure interaction component over the training data, or other specified data distribution, divided by the standard deviation of the corresponding target function

$$S(\{j\}_1^n) = \sqrt{\text{var}_{\mathbf{x}}[I(\{x_j\}_1^n)] / \text{var}_{\mathbf{x}}(F(\mathbf{x}))}. \quad (28)$$

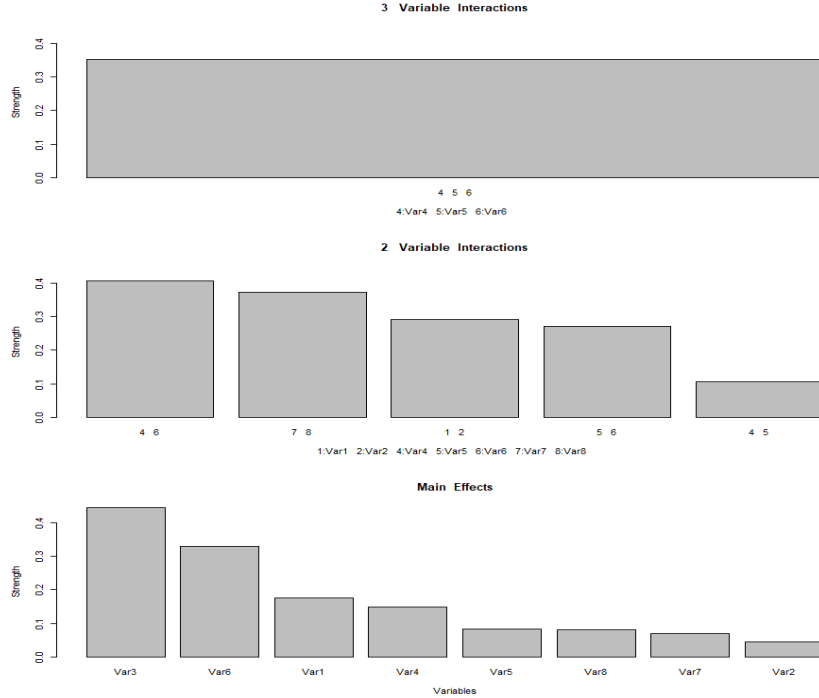


Figure 3: Strengths of identified main and interaction effects in the synthetic data example of Section 3.

If there exists a higher order interaction effect jointly involving variables in subset $\{x_j\}_1^m$ along with other variables $\{x_j\}_{m+1}^n$, $S(\{j\}_1^m) > 0$ (28), then the form of the interaction function of the subset $I(\{x_j\}_1^m | \{x_j\}_{m+1}^n)$ depends on the joint values of the complement variables $\{x_j\}_{m+1}^n$. The resulting unconditioned interaction effect $I(\{x_j\}_1^m)$ is then an average over the joint distribution $p(\{x_j\}_{m+1}^n)$ of the complement variables. If there are no such higher order interactions involving $\{x_j\}_1^m$ jointly with other variables, its pure interaction effect $I(\{x_j\}_1^m)$ does not depend on the data distribution $p(\mathbf{x})$ and reflects only properties of the target function $F(\mathbf{x})$.

The measure $S(s)$ (28) indicates the strength of an n -variable interaction effect involving the corresponding variable subset $s = \{x_j\}_1^n$ over the distribution $p(\mathbf{x})$. One can search for substantial interaction effects by evaluating (26–28) over all variable subsets s up to some maximum size $|s| \leq M$. This approach can in principle be applied to a target function $F(\mathbf{x})$ represented in any form. All that is required to compute partial dependence functions is the value of the function at various specified values of \mathbf{x} .

Figure 3 shows the strengths (28) of all interaction effects uncovered in the synthetic data example of Section 3 using this approach. The presence of more lower order interaction effects shown here than explicitly represented by the function tree (Fig. 1) is due to lower level marginals of higher order basis functions (9) being assigned to their proper interaction level.

5 Computation

For a total of p variables the number of distinct subsets involving $n < p$ variables is $\binom{p}{n}$. For each such subset the number of partial dependence functions required to extract its pure interaction effect (26) (27) grows exponentially in its size n . Thus for larger values of p and n the required computation using the standard method (18) to evaluate all of the necessary partial dependence functions is generally too severe to allow a search for interaction effects by complete enumeration over all variable subsets. However, for functions represented by a function tree, one can employ

(20) to dramatically reduce the computation (21) required to evaluate each partial dependence function. This in turn allows the search for interactions to be performed over many more and larger variable subsets representing higher order interaction effects.

For small to moderate number of variables $p \lesssim 20$ complete enumeration using (20) is generally feasible for $n \lesssim 4$. However, for larger problems the rapid growth with respect to both p and n soon places the required computation out of reach. Parallel computation and smart strategies for reusing previously computed partial dependence functions can somewhat ease this burden. However, the properties of partial dependence functions allow a simple input variable screening approach that can often considerably reduce the size of the search.

If for a (centered) function $F(\mathbf{x})$ a variable x_j participates in no interactions with any other variables then it can be expressed as

$$F(\mathbf{x}) = PD(x_j) + PD(\mathbf{x}_{\setminus j}) \quad (29)$$

where $PD(x_j)$ is its partial dependence on x_j and $PD(\mathbf{x}_{\setminus j})$ is its partial dependence on all other variables (Friedman and Popescu 2008). One can define an overall interaction strength for each predictor variable as

$$H_j = \sqrt{\hat{E}_{\mathbf{x}}(F(\mathbf{x}) - PD(x_j) - PD(\mathbf{x}_{\setminus j}))^2}. \quad (30)$$

Variables x_j with small values of H_j can be removed from the search for interaction effects. This often excludes many variables thereby substantially reducing computation.

Computation can be further reduced by taking advantage of the function tree representation. The function tree strength of the contribution of input variable x_j to interaction level k is taken to be

$$R_{jk} = \sum_{m=1}^M I(j \in m) I(int(B_m) = k) \sqrt{var_{\mathbf{x}}[B_m(\mathbf{x})]}. \quad (31)$$

Here $I(\cdot)$ is an indicator of the truth of its argument, m labels a node of the M node function tree, $B_m(\mathbf{x})$ is its corresponding basis function, $int(B_m)$ its interaction order and the variance is over the distribution $p(\mathbf{x})$. This can be used as a filter to exclude variables x_j with small values of R_{jk} (31) from the search for k -variable interaction effects. Since node basis functions $B_m(\mathbf{x})$ are not pure interaction effect functions (26) (27) the search for n -variable interaction effects should include the union of all relevant variables with substantial contributions (31) at that interaction level or higher.

In many applications the number of variables involved in higher order interactions is less than that involved in main or lower order interaction effects. Since computation increases very rapidly with the number of variables examined, further variable reduction at the interaction level (31) can substantially reduce computation even for minor variable reductions.

For the simulation example in Section 6.2 (below) exhaustive search over all 30 variables at each of four interaction levels requires computing 2027970 partial dependence functions with 2.03×10^{12} corresponding target function evaluations using (18) with $N = N_{\mathbf{z}} = 1000$. This would take approximately 36 days on a Dell XPS 13 laptop. Approximating the search by only including the ten variables estimated to be the most important reduces the necessary number of partial dependence functions to 15540 requiring 1.55×10^{10} target function evaluations. This would take approximately seven hours.

Partial dependence screening using (30) identifies six interacting variables reducing the number of partial dependence functions computed to 1114 with 1.11×10^9 target function evaluations using (18). This reduces the computing time to approximately 30 minutes. Building the function tree for this example required 14.5 seconds. Corresponding interaction level screening using (31) eliminated all four-variable interactions. Six variables remained for both the two-variable and three-variable interaction searches and ten variables for main effects. This requires a total of 384 partial dependence functions. Employing (20) with $N = N_{\mathbf{z}} = 1000$ involved 4.14×10^5 target function evaluations requiring 0.5 seconds.

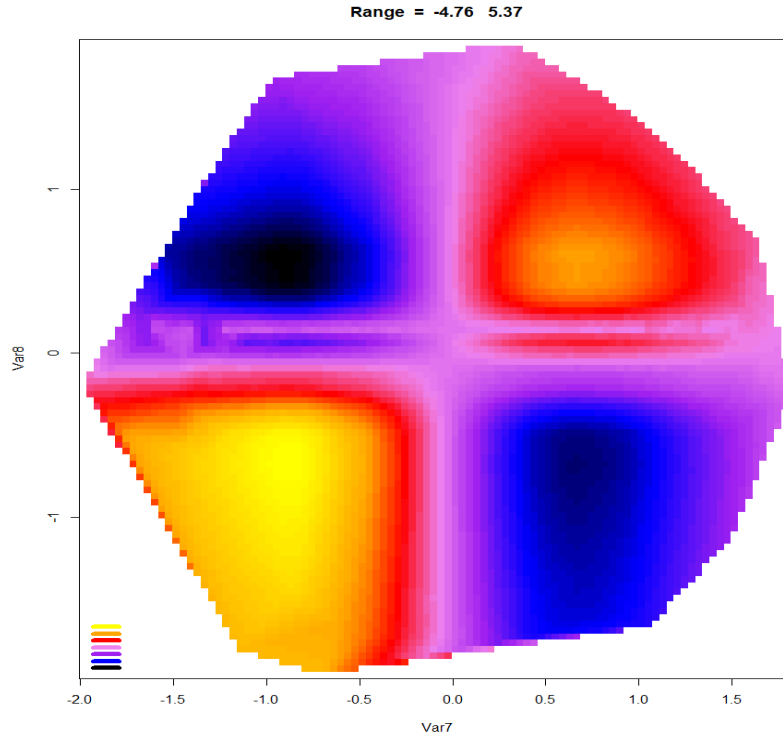


Figure 4: Interaction effect of variables x_7 and x_8 on simulated data example of Section 3.

5.1 Interaction investigation

Once discovered, interactions as well as main effects can be visualized using partial dependence plots. Figure 4 shows a heat map representation of the interaction effect between variables x_7 and x_8 , $I(x_7, x_8)$ (26) (27), for the function tree model $\hat{F}(\mathbf{x})$ (Figs. 1 & 2). Colors black, blue, purple, violet, red, orange, and yellow, seen in the lower left legend, represent a continuum of increasing function values from lowest (-5.06) to highest (5.49).

One sees that joint high or joint low values of these two variables produce relatively large increases in function value (red, yellow), whereas opposite values, (low, high) or (high, low), give rise to large decreases (blue, black). Since Fig. 3 shows no higher order interactions involving these variables, this function of x_7 and x_8 represents the corresponding interaction effect associated with the target function estimate $\hat{F}(\mathbf{x})$, and does not reflect the nature of the data distribution $p(\mathbf{x})$. One can verify this behavior by examining the true target function (10).

Variables x_4 and x_5 are seen in Fig. 3 to have a relatively weak interaction. However, they are also seen to participate in a substantial three-variable interaction with variable x_6 so that their two-variable interaction function $I(x_4, x_5)$ (26) (27) may not provide a complete description of their joint effect on the target estimate $\hat{F}(\mathbf{x})$.

Figure 5 shows a plot of the average (unconditional) pure interaction function $I(x_4, x_5)$ (upper left), and corresponding interaction functions $I(x_4, x_5 | x_6)$ conditioned at three values of $x_6 \in \{-2, 0, 2\}$, all plotted on the same vertical scale ($-63, 63$). Here a black color represents the most negative values, yellow the most positive and violet the smallest absolute values. The upper left frame shows that the variation of unconditional interaction function $I(x_4, x_5)$ is quite small (\simeq violet) as indicated in Fig. 3. The lower left frame shows the same for $I(x_4, x_5 | x_6 = 0)$. The two right frames however show very strong interaction effects for $I(x_4, x_5 | x_6 = -2)$ and $I(x_4, x_5 | x_6 = 2)$. There is almost no interaction between x_4 and x_5 when $x_6 = 0$. For $x_6 = \pm 2$, there are strong but *opposite* interaction effects. This leads to an overall weak two-

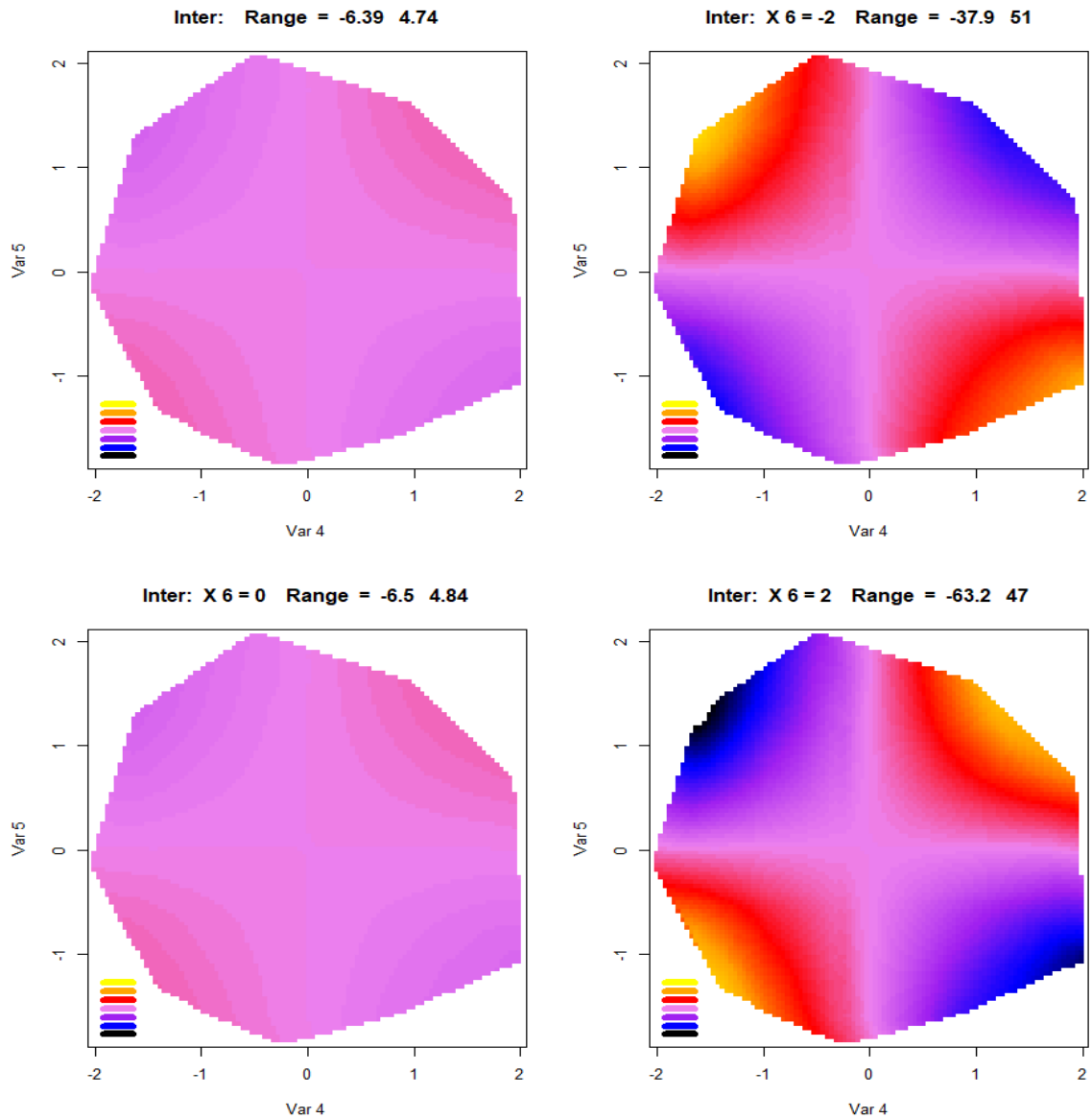


Figure 5: Average interaction effect $I(x_4, x_5)$ on variables x_4 and x_5 (upper left), conditioned $I(x_4, x_5 | x_6)$ on $x_6 = -2$ (upper right), $x_6 = 0$ (lower left) and $x_6 = 2$ (lower right) for simulated data of Section 3.

variable interaction between x_4 and x_5 when averaged over the distribution of x_6 (upper left). Seeing only this weak two-variable interaction effect between (x_4, x_5) without knowledge of the corresponding three-variable (x_4, x_5, x_6) interaction would lead to the impression that these two variables influence the target $F(\mathbf{x})$ in an additive unrelated manner. As seen in the right two frames of Fig. 5 this is clearly not the case. Thus, in the presence of higher order interactions, lower order representations can be misleading.

6 Illustrations

The function tree methodology described above was applied to a number of popular public data sets to investigate the nature of the relationship between the joint values of their predictor variables and outcome. In many cases the corresponding function tree uncovered simple relationships involving additive effects or at most a few two-variable interactions. Others were seen to involve more complex structure. Examples of both are illustrated here.

The goal of the function tree approach is interpretational. As such its form (7) (8) is somewhat more restrictive than other more flexible methods focused purely on prediction accuracy such as XGBoost (Chen and Guestrin 2016) or Random Forests (Breiman 2001). However, if on any particular problem its accuracy is substantially less than these other methods the quality of the corresponding interpretation may be questionable. For each of the examples presented in this section root-mean-squared prediction error

$$RMSE = \sqrt{\frac{\sum_{i=1}^N (y_i - \hat{F}(\mathbf{x}_i))^2}{\sum_{i=1}^N (y_i - \bar{y})^2}} \quad (32)$$

is reported for default versions of the three methods: no tuning for Random Forests and only model size tuning for function trees and XGBoost. In all examples presented here the estimated interaction effects are based on partial dependence functions (Section 4.1). Corresponding summaries using partial association functions (Section 4.2) produced nearly identical results in all cases.

6.1 Capital bikeshare data

This data set taken from the UCI Machine Learning Repository consists of 17379 hourly observations of counts of bicycle rentals in the Capital bikeshare system in Washington, D. C. between 2011 and 2012. The outcome variable y is the rental count. The sixteen predictor variables are both categorical and numeric consisting of corresponding time, weather and seasonal information.

Figure 6 displays the tree for the function tree model and Fig. 7 shows the corresponding node functions. Its interaction effect summary is shown in Fig. 8. Figure 8 indicates existence of substantial two-variable and three-variable interactions. An important question is the extent to which these effects are properties of the target function and not just properties of a particular training sample. A way to address this is through a bootstrap analysis (Efron 1979). Figure 9 shows box plots of the distributions over fifty bootstrap replications of test set root-mean squared-error (32) of function tree models built under three constraints on maximum interaction order: unconstrained (left), no three-variable interactions allowed (center), and no interactions allowed (right). As seen, existence of both two-variable and three-variable interactions are significant.

The largest estimated two-variable interaction effect is between variables hour-of-day (hr) and the binary indicator for working/non-working days (wrk). Figure 10 shows the partial dependence of DC bike rentals on time-of-day conditioned on working days $wrk = 1$ (top) and non working days $wrk = 0$ (bottom). They are seen to be quite different indicating a strong interaction effect between these two variables. In particular, the sharp reduction in rentals

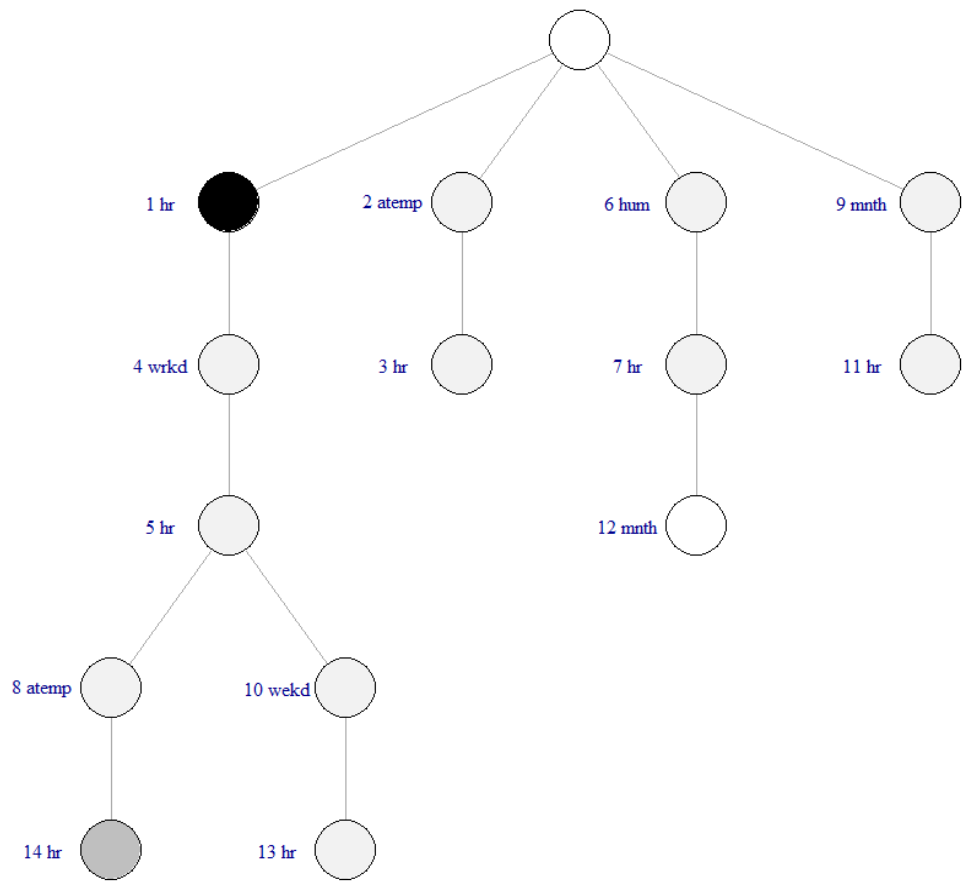


Figure 6: D. C. bicycle rental model function tree.

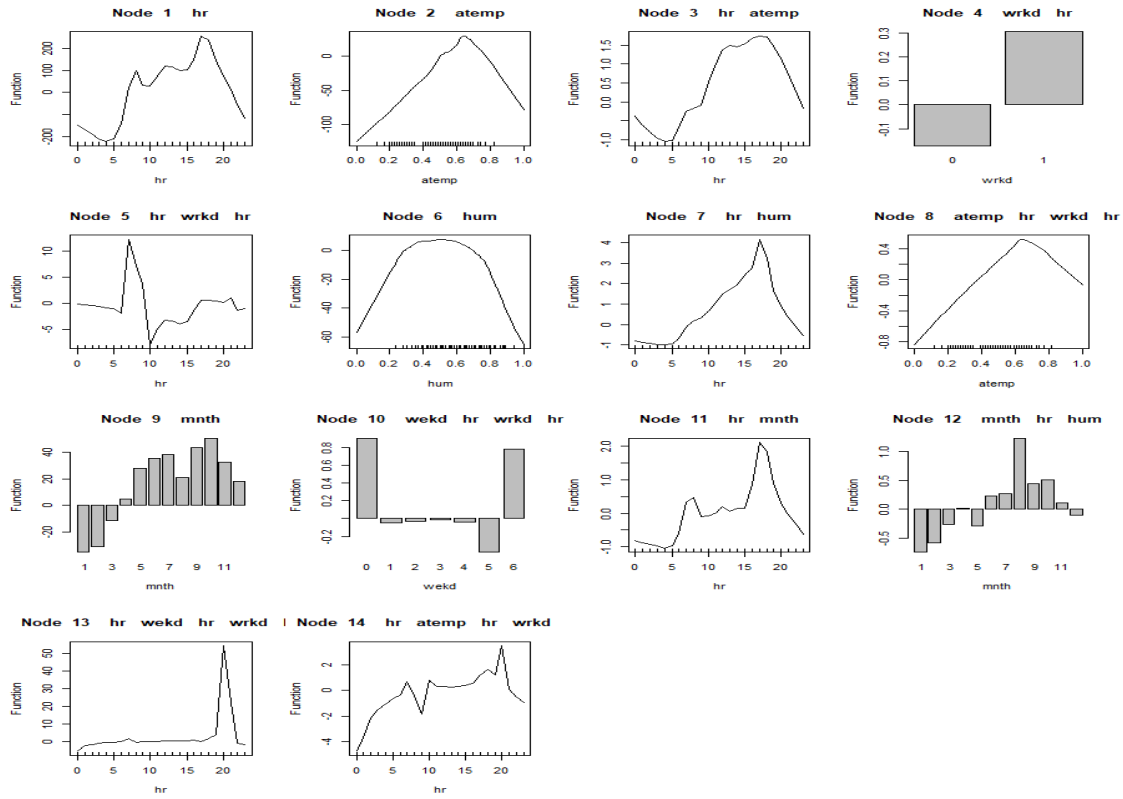


Figure 7: Node functions for bicycle rental function tree.

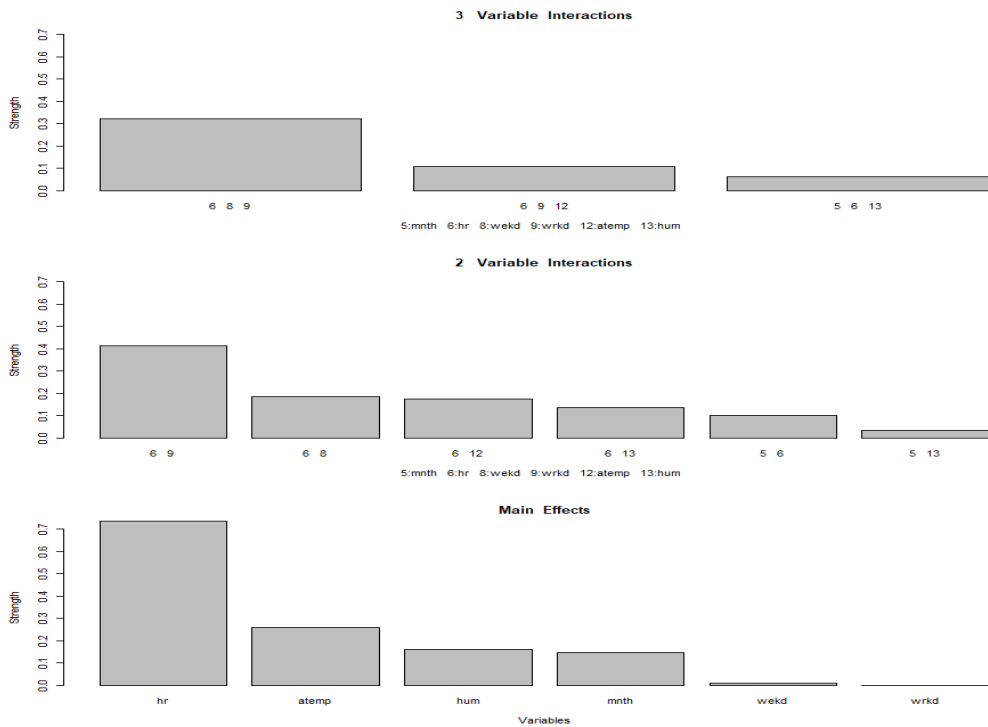


Figure 8: Interaction effect summary for bicycle rental function tree.

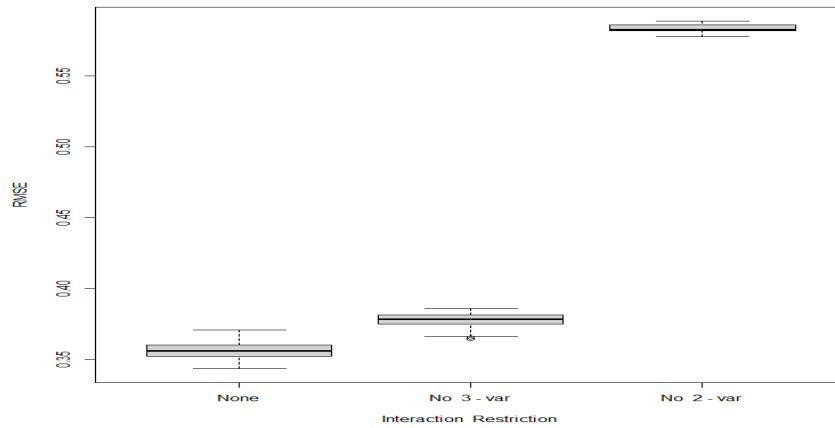


Figure 9: Boxplots of the distributions over 50 bootstrap replications of test set root mean squared error of three function tree models on the bike rental data: unconstrained (left), only main and two-variable interactions (middle), and only main effects (right).

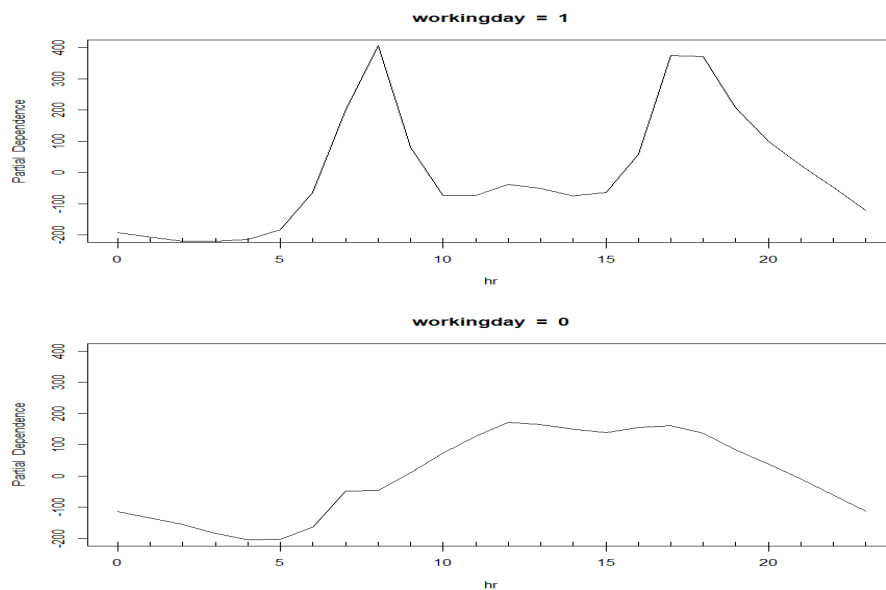


Figure 10: Partial dependence of DC bike rentals on time-of-day for working days (top) and non working days (bottom).

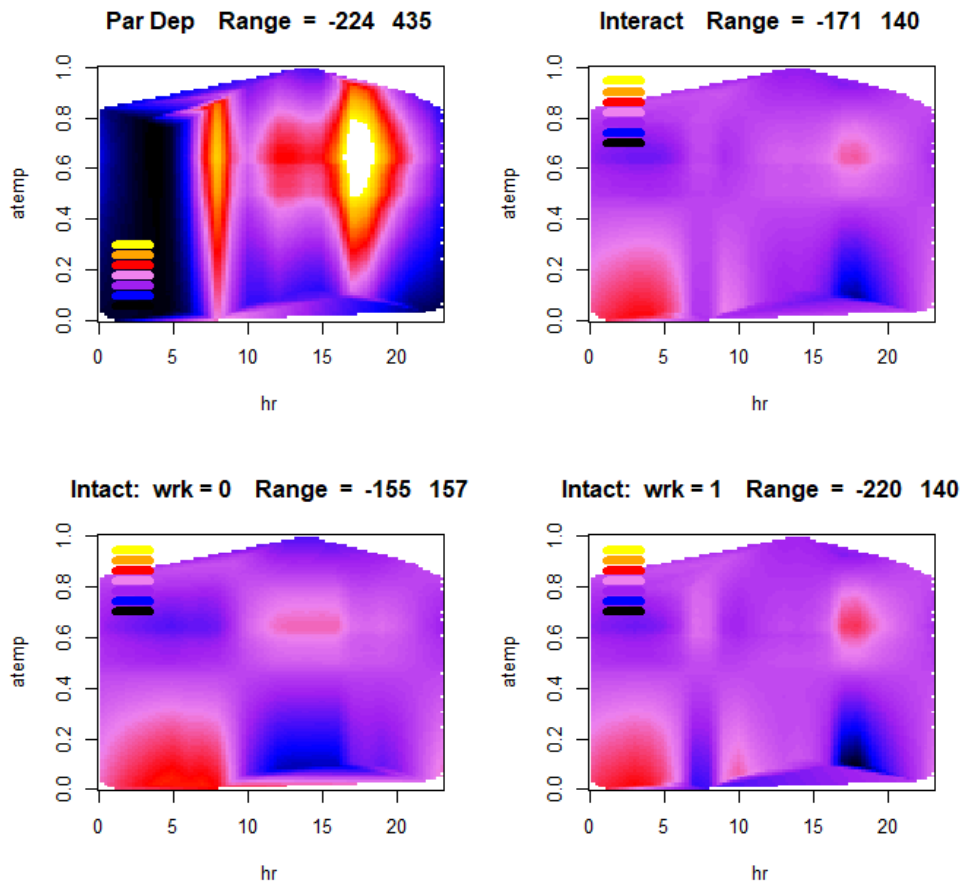


Figure 11: Partial dependence $PD(atemp, hr)$ of bike rentals jointly on adjusted temperature and time-of-day (upper left), its pure interaction component $I(atemp, hr)$ (upper right) and the pure interaction effect separately conditioned on the value of working day $wrk = 0$ (lower left) and $wrk = 1$ (lower right)

beginning at 8am and continuing until 5pm on working days is seen not to exist on non-working days.

The upper left frame of Fig. 11 shows the partial dependence of bike rentals jointly on adjusted temperature ($atemp$) and time-of-day (hr), along with its pure interaction component $I(hr, atemp)$ (top right). Figure 8 indicates a three-variable interaction between variables hour (hr), working day indicator (wrk) and adjusted temperature ($atemp$). Thus, the nature of the interaction effect between hr and $atemp$ may depend on the value of wrk . The bottom two frames of Fig. 11 show this interaction effect separately conditioned on the value of working day $I(hr, atemp | wrk = 0)$ and $I(hr, atemp | wrk = 1)$. One sees substantial difference in the nature of this interaction for the different values of wrk reflecting the presence of the three-variable interaction.

Figure 8 indicates that the strongest three-variable interaction effect involves the working day indicator (wrk), day of the week ($wekd$) and hour of the day (hr). This is illustrated in Fig. 12. The interaction function $I(wekd, wrk | hr)$ is displayed for $hr \in \{midnight, 6 am, noon, 6 pm\}$. Note that there are no observations for which Saturday ($wekd = 7$) and Sunday ($wekd = 1$) are labeled as working days ($wrk = 2$). The absence of a three-variable interaction would imply that $I(wekd, wrk | hr)$ is the same for all values of the variable hr . As seen in Fig. 12 this is not the

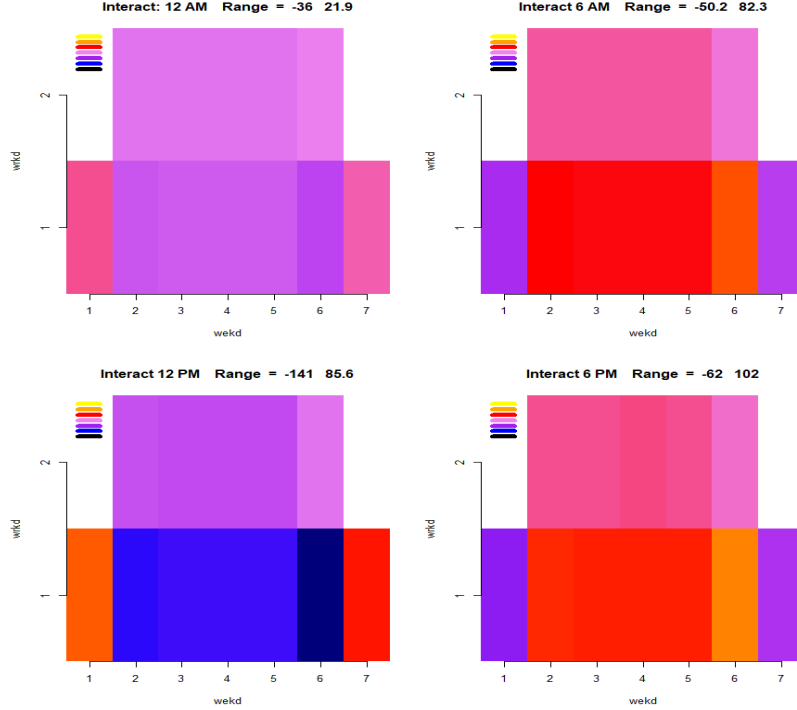


Figure 12: Bike data Interaction effect $I(\text{wekd}, \text{wrk} | \text{hr})$ for $\text{hr} \in \{\text{midnight}, 6\text{am}, \text{noon}, 6\text{pm}\}$.

case especially for non working weekdays at noon (lower left).

The $RSME$ (32) of function tree, XGBoost and Random Forest models on this example was 0.34, 0.37 and 0.38, respectively.

6.2 Simulated data

This example was presented in Hu *et. al.* (2023). They generated data using the target function

$$g(\mathbf{x}) = \sum_{j=1}^5 x_j + 0.5 \sum_{j=6}^8 x_j^2 + \sum_{j=9}^{10} x_j I(x_j > 0) + x_1 x_2 + x_1 x_3 + x_2 x_3 + 0.5 x_1 x_2 x_3 + x_4 x_5 + x_4 x_6 + x_5 x_6 + 0.5 I(x_4 > 0) x_5 x_6. \quad (33)$$

This is a function of ten variables involving numerous interactions involving up to three variables. The response was simulated as

$$y = g(\mathbf{x}) + \varepsilon, \quad \varepsilon \sim N(0, 0.5^2). \quad (34)$$

There were 30 predictor variables. The first 20 were simulated from a multivariate Gaussian distribution with mean 0, variance 1 and equal correlation 0.5 between all pairs. Ten additional variables were included that were independent of the first 20 (irrelevant variables). They were also simulated from a multivariate Gaussian distribution with mean 0, variance 1 and equal correlation 0.5 between all pairs. All predictors were truncated to be within the interval $[-2.5, 2.5]$. Here the sample size was taken to be $N = 20000$.

Figure 13 shows the largest estimated main and interaction effect strengths up through four-variables. One sees that all of the main and interaction effects represented in (33) are shown with substantial strengths. Those not represented in (33), including all four-variable interactions, either do not appear or do so with very low estimated strength.

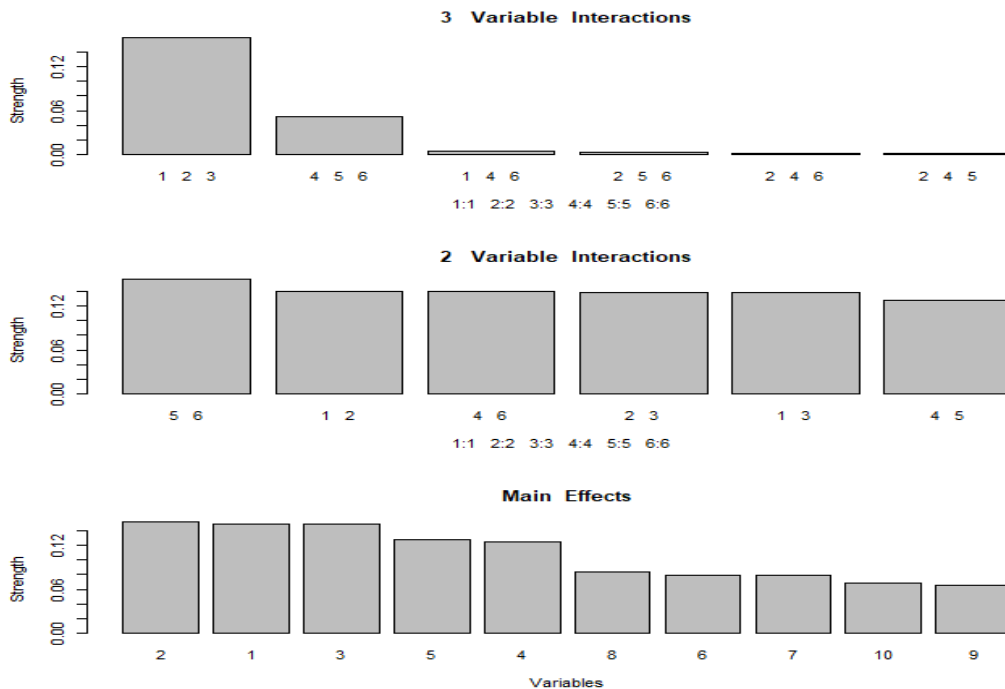


Figure 13: Strengths of main and interaction effects identified in the simulated data example of Section 6.2.

The $RSME$ (32) of function tree, XGBoost and Random Forest models on this example was 0.062, 0.147 and 0.174 respectively.

6.3 Pumadyn data

The other examples were chosen to represent data with somewhat complex target function structure. Here we illustrate on a data set where the function tree uncovers very simple structure. The data (Corke 1996) is produced from a realistic simulation of the dynamics of a Puma 560 robot arm. The task is to predict the angular acceleration of one of the robot arm’s links. There are 8192 observations involving 32 input variables that include angular positions, velocities and torques of the robot arm.

Figure 14 shows the resulting entire function tree model. The upper left frame shows the tree and the other frames show the node functions. Figure 15 shows the (only) interaction effect between τ_4 and θ_5 . The upper left frame shows the partial dependence function $PD(\theta_5, \tau_4)$; upper right frame shows its additive component and lower left frame its pure interaction effect $I(\theta_5, \tau_4)$. The lower right frame represents $I(\theta_5, \tau_4)$ as a perspective mesh plot. Of the 32 input variables, the function tree model selected only two of them to explain 97% of the variance of the target.

The $RSME$ (32) of function tree, XGBoost and Random Forest models on this example was 0.18, 0.21 and 0.27, respectively.

6.4 SGEMM GPU kernel performance

This data set from the UCI Machine Learning Repository measures the running time required for a matrix-matrix product using a parameterizable SGEMM GPU kernel. There are 241600 observations with 14 predictor variables:

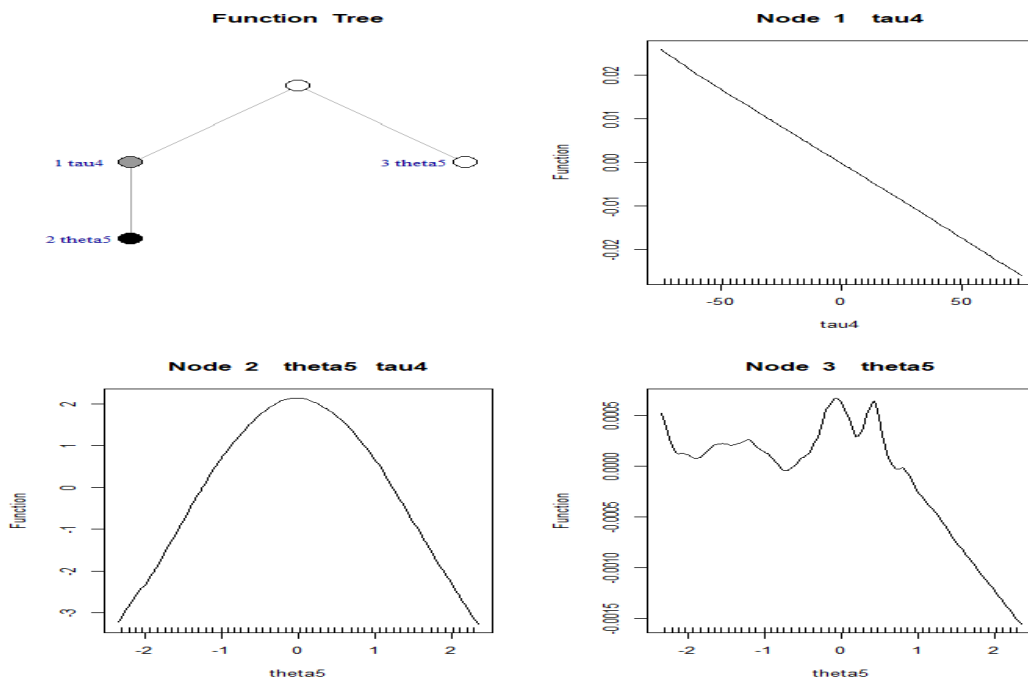


Figure 14: Function tree model resulting from the Pumadyn data with the tree (upper left) and respective node functions.

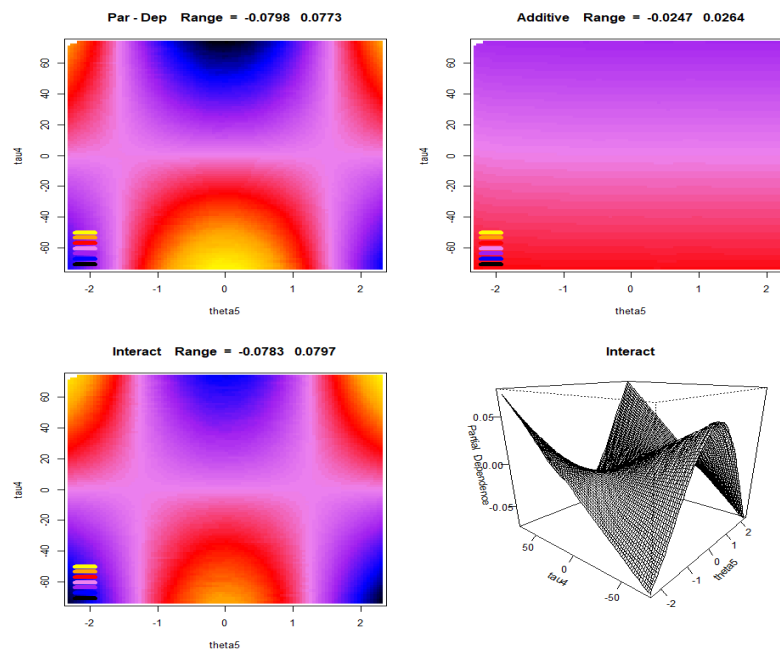


Figure 15: Pumadyn data: partial dependence on variables τ_4 and θ_5 (top left), additive contribution (top right), pure interaction (bottom left) and pure interaction perspective mesh plot (bottom right).

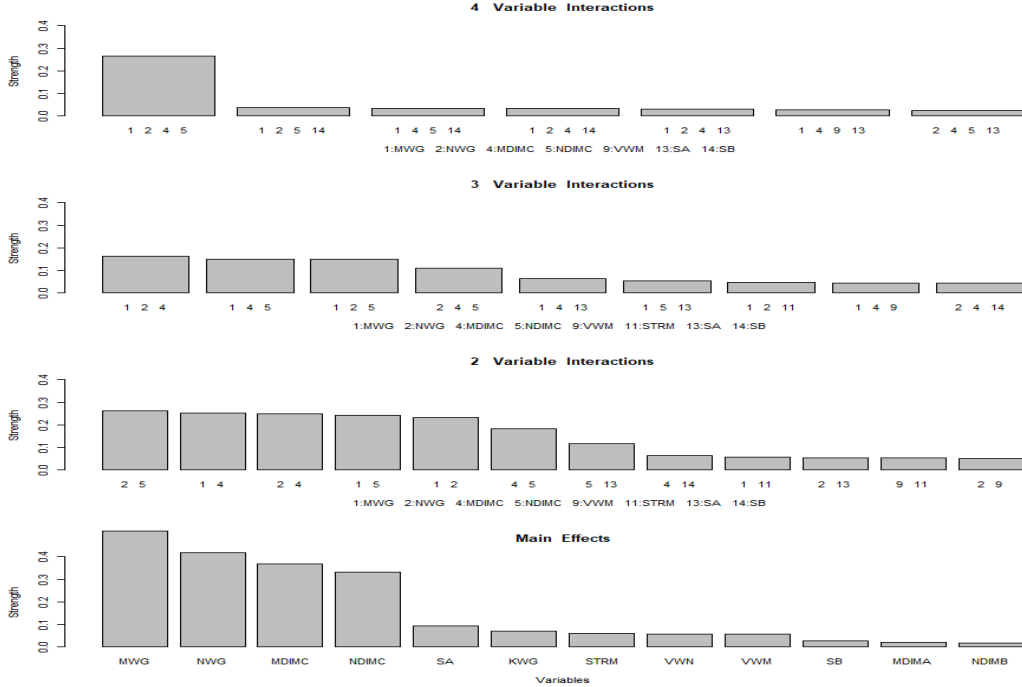


Figure 16: Strengths of main and interaction effects identified in the SGEMM GPU kernel performance data.

SGEMM GPU kernel performance predictor variables

1-2	<i>mwg, nwg</i>	per-matrix 2Dtiling at workgroup level
3	<i>kwg</i>	inner dimension of 2Dtiling at workgroup level
4-5	<i>mdimc, ndimc</i>	local workgroup size
6-7	<i>mdima, ndimb</i>	local memory shape
8	<i>kwi</i>	kernel loop unrolling factor
9-10	<i>vwm, vwn</i>	per-matrix vector widths for loading and storing
11-12	<i>strm, strn</i>	enable stride for accessing off-chip memory within a single thread
13-14	<i>sa, sb</i>	per-matrix manual caching of the 2D workgroup tile.

As suggested by the authors, the outcome was taken to be the logarithm of the running time. All predictor variables realize at most four distinct values and were therefore treated as being categorical. Figure 16 shows the estimated interaction effect profile for this data. Among the larger effects are four main, seven two-variable, four three-variable and a large four-variable interaction effect.

Figure 17 shows box plots of the distributions over ten bootstrap replications of test set root-mean squared-error (32) of function tree models built under three interaction constraints: unconstrained (left), four-variable interaction among variables (*mwg, nwg, mdimc, ndimc*) prohibited (center), and all four-variable interactions prohibited (right). Note that not allowing the four-variable interaction among (*mwg, nwg, mdimc, ndimc*) does not preclude any of these variables from participating in lower order interactions, or four-variable interactions with other variables. One sees that incorporating the (*mwg, nwg, mdimc, ndimc*) four-variable interaction is very important to model accuracy as are other four-variable interactions to a lesser extent.

Since the (*mwg, nwg, mdimc, ndimc*) interaction effect is inherently four dimensional it cannot be completely represented by a two dimensional display. Unlike three-variable interactions it cannot be represented by a series of two dimensional plots conditioned on the value of a third

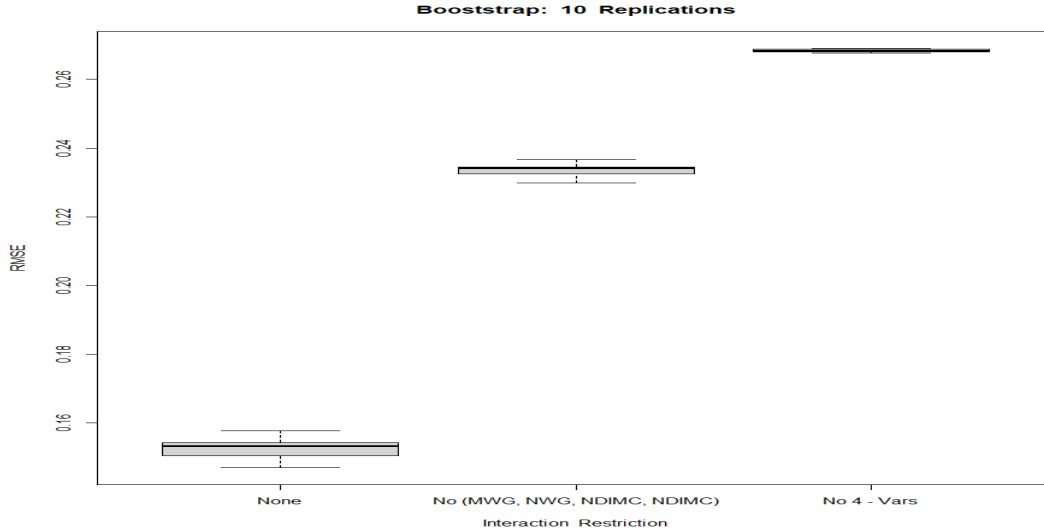


Figure 17: Boxplots of the distributions over 10 bootstrap replications of test set root mean squared error of three function tree models on the GPU performance data: unconstrained (left), no ($mwg, nwg, mdimc, ndimc$) interaction (center), and no four variable interactions (right)

variable. However it is possible to gain some insight about this four-variable interaction effect through graphical methods.

Figure 18 depicts the difference between interaction effects computed from two models

$$\hat{D}(\mathbf{x}) = \hat{F}(\mathbf{x}) - \hat{G}(\mathbf{x}). \quad (35)$$

The first $\hat{F}(\mathbf{x})$ is the full model with all interactions allowed (Fig. 17 left). The second model $\hat{G}(\mathbf{x})$ was built under the constraint that no four-variable interaction effect among variables ($mwg, nwg, mdimc, ndimc$) was allowed (Fig. 17 center). Thus, any structure detected in $\hat{D}(\mathbf{x})$ is due to presence of this four-variable interaction.

Figure 18 shows nine bivariate interaction effects differences between these two models (35)

$$I_{\hat{D}}(mwg, nwg | mdimc \in \{8, 16, 32\} \times ndimc \in \{8, 16, 32\})$$

where $mwg, nwg \in \{16, 32, 64, 128\}$. For the top two rows $mdimc \in \{8, 16\}$, the model differences are seen to be small in absolute value (\simeq violet) for all joint values of the other variables, indicating that the four-variable interaction has little to no effect for those collective values. For the last row ($mdimc = 32$) one sees that the absolute differences are larger (red, yellow, blue), especially for $ndimc = 32$. This four-variable interaction effect is seen to be mainly the result of a very large increase in (log) running time for the GPU matrix product when simultaneously $mdimc$ and $ndimc$ realize their largest values while at the same time mwg and nwg are at their smallest values.

The $RSME$ (32) of function tree, XGBoost and Random Forest models on this example was 0.12, 0.09 and 0.16, respectively.

6.5 Global surrogate

Function trees can be used as interpretable surrogate models to investigate the predictions of black box models. One simply uses the black box predictions along with the corresponding predictor variables as input. To the extent that the function tree fit is accurate, all of its interpretational tools can then be applied to study the nature of the black box model. This is

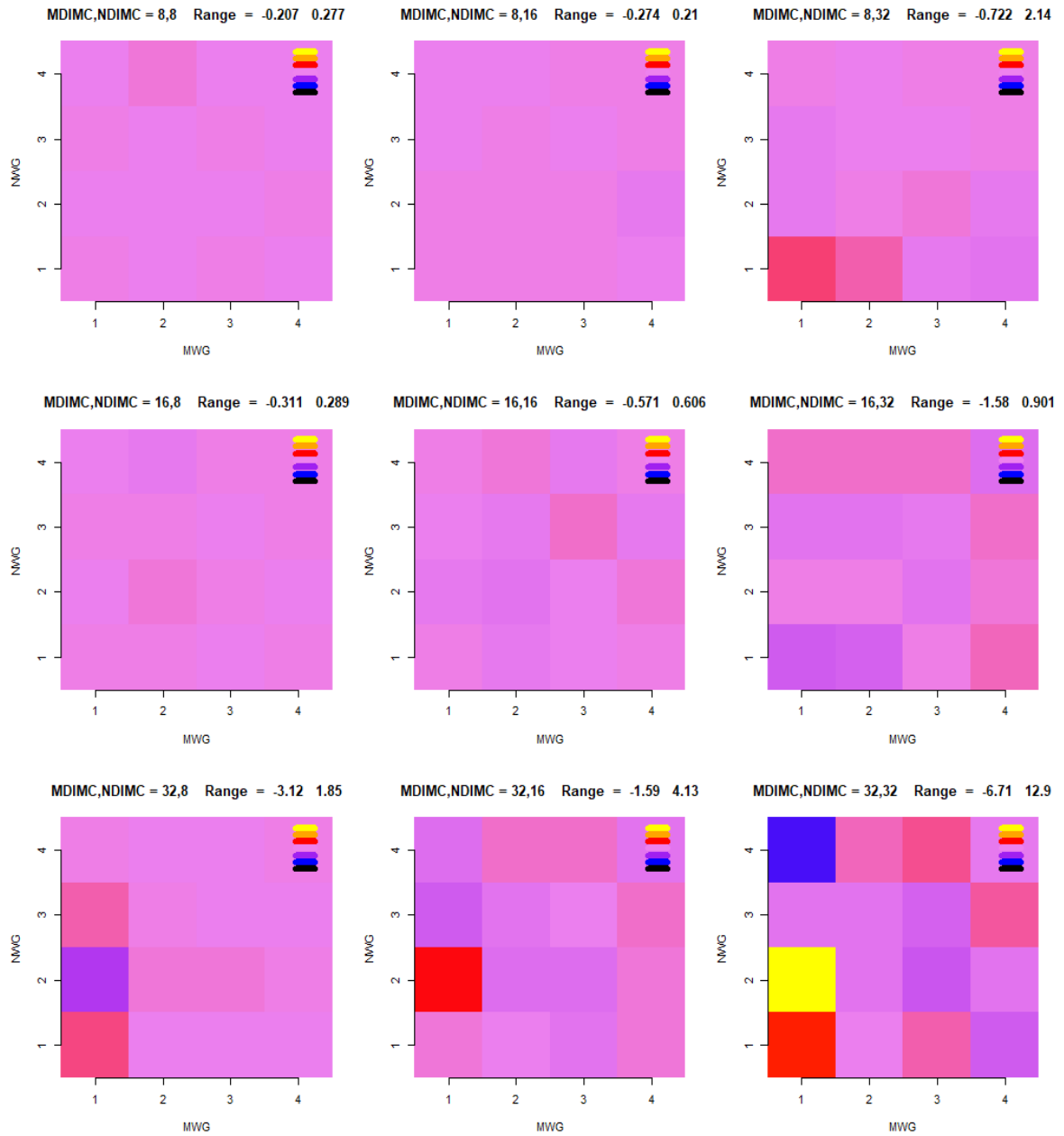


Figure 18: SGEMM GPU kernel interaction effect differences with and without the $(mwg, nwg, mdimc, ndimc)$ four-variable interaction effect.

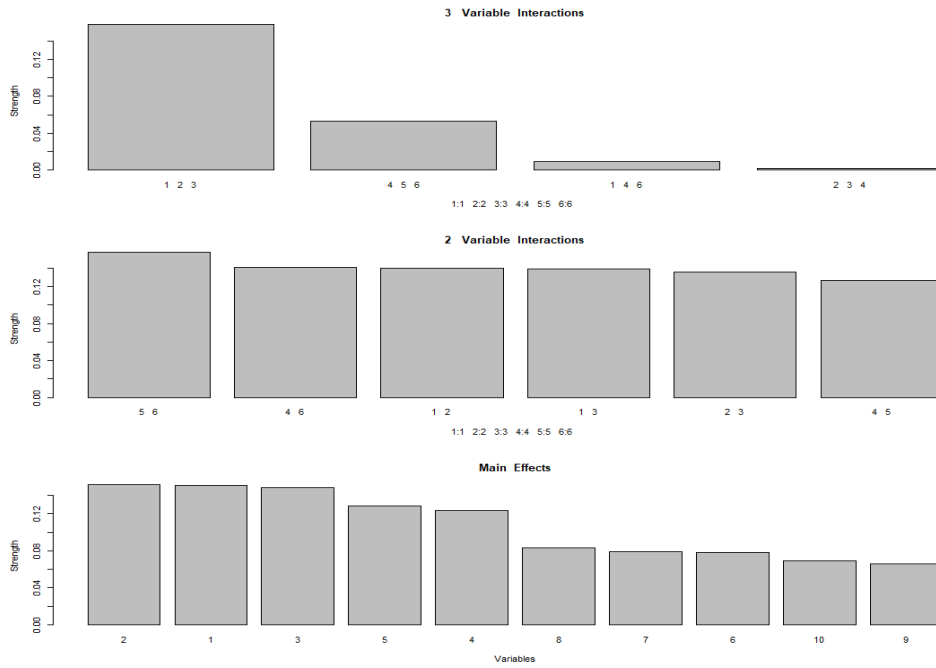


Figure 19: Strengths of main and interaction effects identified in the XGBoost regression model on the simulation data of Section 6.2

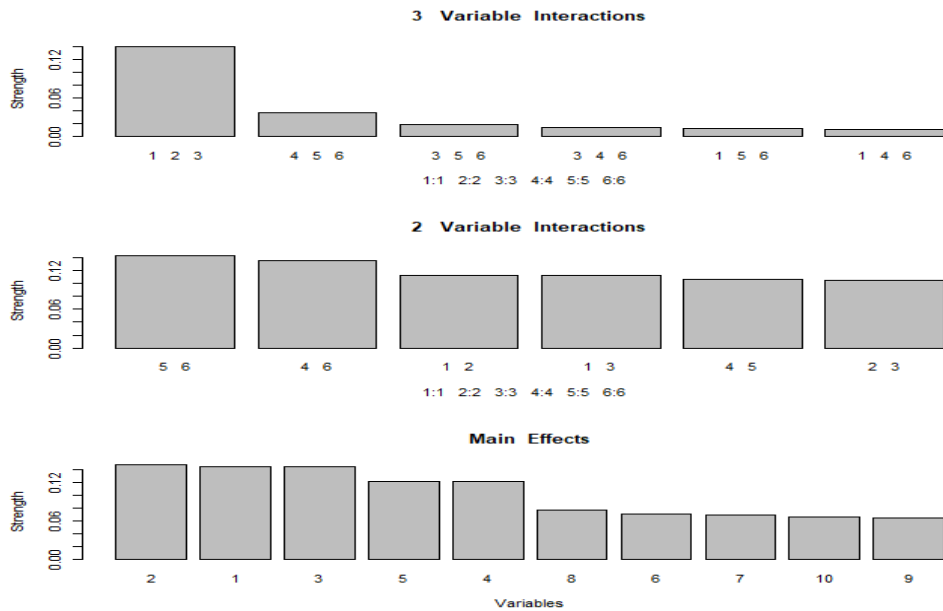


Figure 20: Strengths of main and interaction effects identified in the Random Forest regression model on the simulation data of Section 6.2

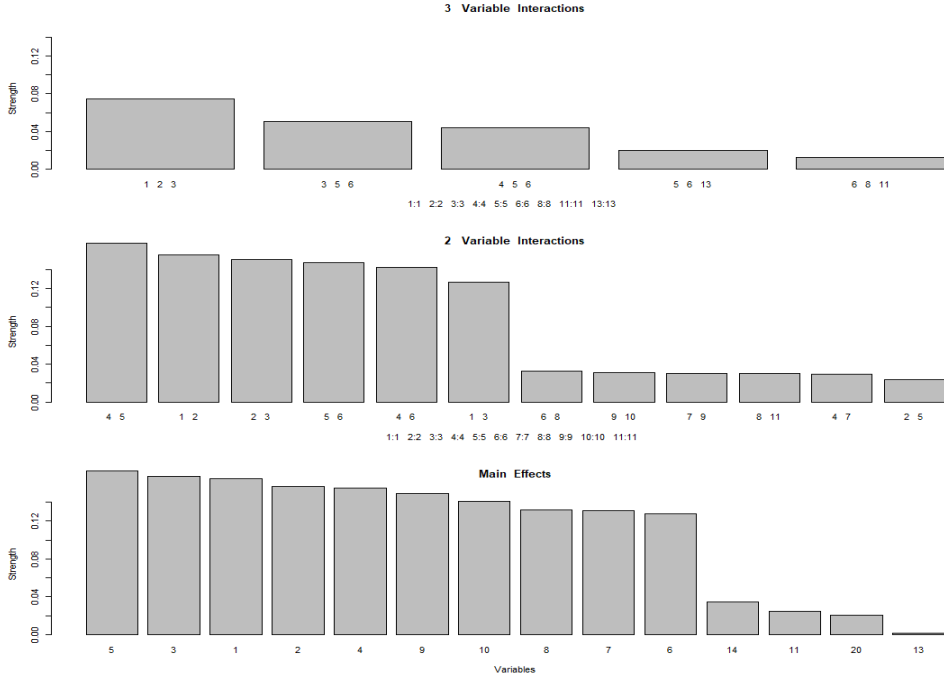


Figure 21: Strengths of main and interaction effects identified in the XGBoost classification model on the simulation data of Section 6.2

illustrated using the simulated data of Hu *et. al.* (2023), shown in Section 6.2, where the true underlying structure (33) is known.

First XGBoost is applied in regression mode to model the data (34) producing an estimate $\hat{g}(\mathbf{x})$. The resulting test data root-mean-squared error

$$RMSE(\hat{g}) = \left\{ \hat{E}_{\mathbf{x}}[(g(\mathbf{x}) - \hat{g}(\mathbf{x}))^2] / Var(g(\mathbf{x})) \right\}^{\frac{1}{2}} \quad (36)$$

was $RMSE(\hat{g}) = 0.14$. The output of the XGBoost model $\hat{g}(\mathbf{x})$ is then fit with a function tree. The $RMSE$ for this fit was 0.13 indicating that the function tree accurately reflects the XGBoost model. Figure 19 displays the resulting largest main and interaction effects detected by the function tree in the XGBoost model. This can be compared to the function tree based on the original data shown in Fig. 13, as well as to the structure of the true target function (33). One sees that the XGBoost regression model here closely captures the true target function structure as reflected in its function tree representation.

Next a Random Forest is applied to the same data. The resulting test data root-mean-squared error (36) was $RMSE(\hat{g}) = 0.17$. The output of this random forest model was fit by a function tree producing a corresponding $RMSE$ of 0.053. Figure 20 shows the largest main and interaction effects detected in the Random Forest model. While capturing the nature of the target function reasonably well, the random forest appears to somewhat under estimate the (x_4, x_5, x_6) interaction strength and identify several spurious three-variable interactions.

Finally here we apply the surrogate approach in a classification setting. The outcome variable is binary, $y \in \{0, 1\}$ with $\Pr(y = 1 | \mathbf{x}) = 1/(1 + \exp(-g(\mathbf{x})))$. The log-odds function $g(\mathbf{x})$ is given by (33). Logistic XGBoost was applied to this (\mathbf{x}, y) data producing a log-odds estimate $\hat{g}(\mathbf{x})$. The resulting root-mean-squared-error $RMSE(\hat{g}) = 0.39$ (36) is in this case much larger owing to the loss of information associated with providing the learning algorithm with only the sign of the outcome rather than its actual numerical value. This logistic XGBoost model was then fit with a function tree with resulting $RMSE$ of 0.19. Although larger than in the regression

case this still represents a fairly close fit ($R^2 = 0.96$). The result is shown in Fig. 21. As would be expected this lower accuracy logistic XGBoost model less perfectly captures the true target function (33). It uncovers all of the true main and interaction effects. It also indicates a number of spurious main and two-variable interactions at somewhat lower strength. The strength of the interaction among variables (x_1, x_2, x_3) is under estimated and there are several spurious three-variable interactions indicated at comparable strength. In spite of its lower accuracy the logistic XGBoost model is still seen in Fig. 21 to reflect much of intrinsic structure of the target log-odds $g(\mathbf{x})$ (33).

7 Previous work

The origins of the function tree approach lie with the additive modeling procedure of Hastie and Tibshirani (1990). They used nonparametric univariate smoothers and backfitting to produce models with no interactions. Function trees can be viewed as generalizing that method to discover and include unspecified interaction effects.

The closest predecessor to function trees is MARS (Friedman 1991). It models a general multivariate function as a sum of products of simple basic univariate functions of the predictor variables and can in principle model interaction effects to high order. The basic univariate function used with MARS is a dReLU (double ReLU)

$$d(x) = a \cdot (t - x)_+ + b \cdot (x - t)_+ \quad (37)$$

characterized by two slope parameters (a, b) and knot location t . The MARS forward stepwise modeling strategy is similar to that used with the function tree approach.

The principal difference between MARS and function trees involves their basic building blocks. MARS employs the simple dReLU (37) at every step. Function trees employ more general functions of the predictor variables $f(x_j)$ estimated by user selected smoothers. This allows customizing of the estimation method to the nature of each individual predictor variable distribution. It also produces more parsimonious models (smaller trees) since many dReLUs (37) can be required to approximate even simple whole curves.

A second difference with MARS is that function trees allow different functions of the *same* variable to appear multiple times in the products of a single basis function (8), as seen in Fig. 6. This provides more flexibility by incorporating stepwise multiplicative as well as additive modeling. Besides increased accuracy this further reduces model size. In addition to being more interpretable, smaller models allow faster computation of their partial dependence functions.

The use of partial dependence functions to uncover interaction effects was proposed by Friedman and Popescu (2008). The innovation here is their rapid identification and computation afforded by the function tree representation. This allows a comprehensive search for all interaction effects up to high orders. Other techniques that have been proposed for interaction detection are mostly based on the functional ANOVA decomposition (see Roosen 1995, Hooker 2004 & 2007, Kim *et. al.* 2009, Lengerich *et. al.* 2020, Hu *et. al.* 2023, and Walters *et. al.* 2023). So far, computational considerations have limited these approaches to two-variable interactions. Lou *et. al.* (2013) use a bivariate partitioning method to screen for two-variable interactions. Tang, *et. al.* (2016) combine the functional ANOVA technique with the polynomial dimensional decomposition to reduce computation with independent variables.

8 Discussion

While sometimes competitive in accuracy with other more flexible methods such as XGBoost and Random Forests, the focus of the function tree approach is on interpretation. The goal is to provide a representation of the target function that exposes its interaction effects and provides a framework for their rapid calculation, especially those involving more than two variables. Almost all research into interaction detection to date has been limited to that involving just two

variables. In fact, in many settings the unqualified term “interaction effect” is meant to refer to two variables only.

Focusing only on two–variable interactions is natural because it reduces the size of the search and once interactions are detected their functional forms are easily examined by traditional graphical methods such as heat maps, contour plots or perspective mesh plots, etc. Higher order interactions involve more variables and their higher dimensional structures are not as easily represented. As illustrated in Figs. 5, 11 and 12, three–variable interactions can be visualized by viewing a series of bivariate interaction plots conditioned on selected values of another variable. As seen in Fig. 18 interactions involving more variables can be investigated by contrasting models with and without those interactions included.

In addition to their direct interpretational value, knowledge of the existence and strengths of higher order interactions can be important as they place interpretational limits on the nature of those of lower order involving the same variables. As noted above, the functional form of an interaction effect involving variables $\{x_j\}_1^n$ depends on the value of another variable, say x_k , if there exists a higher order interaction involving both $\{x_j\}_1^n$ and x_k . If there are no such substantial higher order interactions, the functional form of the $\{x_j\}_1^n$ interaction is well defined and represents the isolated joint contribution of those variables to the target function. If such higher order interactions do exist then the form of the $\{x_j\}_1^n$ interaction is not well defined as it depends on the value of x_k and its corresponding functional form becomes an average over the joint distribution of all such variables. As seen for example in Fig. 5, this can lead to highly misleading interpretations. Tan *et. al.* (2023) discuss problems interpreting lower order effects in the presence of higher order interactions.

In applications involving training data with very large absolute correlations among subsets of predictor variables, main and interaction effects of various levels involving those variables tend not to be separable. This can cause substantial spurious interaction effects to be reported. These can be detected by comparing the lack-of-fit (32) for models constructed with and without the questionable effects included, as illustrated in Figs. 9 and 17.

A popular interpretational tool used to investigate predictive models is a measure of the impact or importance of the respective individual input variables on model predictions. There are a wide variety of definitions for variable importance each providing different information. See Molnar (2023) for a comprehensive survey. In the presence of interactions the contribution of a given predictor variable depends on the values of the other variables with which it interacts. Interaction effect summaries (e.g. Figs. 8, 13 and 16) are thus more comprehensive than corresponding variable importance summaries. Variable importances can be derived from interaction based functional decompositions. For example, Gevaert and Saeys (2022) and Walters *et. al.* (2023) use them to derive Shapley (1953) values.

In the examples presented here partial dependence functions were used to both detect and examine interaction effects. Computational considerations largely dictate their use for the former. However, once uncovered, identified main and interaction effects can be examined by any appropriate method. For example, accumulated local effects (ALE) functions (Apley and Zhu 2020) can be employed for this purpose. Also, partial dependence based search results can be used to guide methods for constructing functional ANOVA decompositions.

References

- [1] Apley, D. and Zhu, J. (2020). Visualizing the effects of predictor variables in black box supervised learning models. *J. Roy. Statist. Soc. Series. B* **4**, 1059–1086.
- [2] Breiman, L. (2001). Random Forests. *Machine Learning*, **45**, 5–32.
- [3] Chen, T. and Guestrin, C. (2016). XGBoost: A scalable tree boosting system. *Proc. 22nd ACM SIGKDD Int. Conf. on Knowledge Discovery and Data Mining*, 785–794.

- [4] Corke, P. I. (1996). A robotics toolbox for MATLAB. *IEEE Robotics and Automation Magazine*, **3**, 24–32.
- [5] Efron, B. (1979). Bootstrap methods: another look at the jackknife. *Ann. Statist.* **7**, 1–26.
- [6] Friedman, J. and Stuetzle, W. (1981). Projection pursuit regression. *J. Amer. Statist. Assoc.* **76**, 817–823.
- [7] Friedman, J. (1991). Multivariate adaptive regression splines. *Ann. Statist.* **19**, 1–67.
- [8] Friedman, J. (2001). Greedy function approximation: a gradient boosting machine. *Ann. Statist.* **29**, 1189–1232.
- [9] Friedman, J., and Popescu, B. (2008). Predictive learning via rule ensembles. *Ann. of Appl. Statist.* **2**, 916–954.
- [10] Gevaert, A. and Saeys, Y. (2022). PDD-SHAP: Fast approximations for Shapley values using functional decomposition, arXiv:2208.12595v1 [cs.LG]
- [11] Hastie, T. and Tibshirani, R. (1990). *Generalized Additive Models*. CRC Press.
- [12] Hooker, G. (2004). Discovering additive structure in black box functions. *Proc. of the 10th ACM SIGKDD Int. Conf. on Knowledge Discovery and Data Mining*.
- [13] Hooker, G. (2007). Generalized functional ANOVA diagnostics for high-dimensional functions of dependent variables. *J. Comp. and Graph. Statist.* **16**, 709–732.
- [14] Hu, L., Nair, V. J., Sudjianto, A., Zhang, A. and Chen, J. (2023). Interpretable machine learning based on functional ANOVA framework: algorithms and comparisons. arXiv:2305.15670 [stat.ML].
- [15] Irizarry, R. A. (2019). *Introduction to Data Science*. Chapman & Hall.
- [16] Kim, Y., Kim, J., Lee, S. and Kwon, S. (2009). Boosting on the functional ANOVA decomposition. *Statistics and Its Interface* **2**, 361–368.
- [17] Lengerich, B., Tan, S., Chang, C., Hooker, G., Caruana, R. (2020). Purifying interaction effects with the functional ANOVA: an efficient algorithm for recovering identifiable additive models. *Proc. 23rd Int. Conf. Artificial Intel. and Statist. (AISTATS)*.
- [18] Lou, Y., Caruana, R., Gehrke, J., Hooker, G. (2013). Accurate intelligible models and pairwise interactions. *Proc. of the 13th ACM SIGKDD Int. Conf. on Knowledge Discovery and Data Mining*.
- [19] Molar, C. (2023). *Interpretable Machine Learning*. Lean Publishing.
- [20] Roosen, C. (1995). Visualization and exploration of high-dimensional functions using the functional ANOVA decomposition. PhD thesis, Statistics, Stanford University.
- [21] Shapley, L. (1953). A value for n-person games. *Contributions to the Theory of Games* **2**(28), 307–317.
- [22] Tan, S., Hooker, G., Koch, P., Gordo, A. and Caruana, R. (2023). Considerations when learning additive explanations for black-box models. *Machine Learning* **112**, 3333–3359.
- [23] Tang, K., Congedo, P. and Abgrall, R. (2016). Adaptive surrogate modeling by ANOVA and sparse polynomial dimensional decomposition for global sensitivity analysis in fluid simulation. *J. Comput. Physics* **314**, 557–589.
- [24] Walters, B., Ortega-Martorell, S., Olier, I., Lisboa, P.J.G. (2023). How to open a black box classifier for tabular data. *Algorithms* **16**, 181.